Distributed Model Predictive Control for multi-zone building energy systems

Maximilian Mork[a,*], André Xhonneux[a], Dirk Müller[a,b]

[a] *Institute of Energy and Climate Research - Energy Systems Engineering (IEK-10), Forschungszentrum Jülich GmbH, Wilhelm-Johnen-Straße, 52425, Jülich, Germany*
[b] *Institute for Energy Efficient Buildings and Indoor Climate, E.ON Energy Research Center, RWTH Aachen University, Mathieustraße 10, 52074, Aachen, Germany*

Abstract

This paper presents a distributed Model Predictive Control (MPC) approach for large-scale, multi-zone building energy systems based on nonlinear Modelica controller models. The method considers both thermal and hydraulic coupling among different building zones. The iterative and parallel distributed optimization approach builds upon an uncooperative approach for thermal coupling using the Nash equilibrium approach and a cooperative approach for the hydraulic coupling using the Alternating Direction Method of Multipliers (ADMM). Apart from thermal coupling through walls, the modeling takes thermal coupling through doors into account using a data-driven approach, which calculates the inter-zone air exchanges based on temperature differences between door-coupled zones. The hydraulic coupling enables consideration of interactions between the zones introduced by a shared, central Heating, Ventilation and Air Conditioning (HVAC) system. The distributed MPC framework is structured in an easy-scalable, plug-n-play composition, where local systems are automatically assigned to the global coordination scheme. The distributed MPC method is applied to a simulative nonlinear case study, consisting of a detailed six-room-building Modelica model considering both thermal and hydraulic interactions. The benefits of the proposed approach are demonstrated and compared against centralized and decentralized control concepts in terms of energy consumption, discomfort and computation time.

Keywords: Distributed Model Predictive Control, multi-zone building, Modelica, building energy system optimization, HVAC, Alternating Direction Method of Multipliers (ADMM), Nash equilibrium, nonlinear optimization, Thermally activated building systems (TABS)

*Corresponding author
Email address: m.mork@fz-juelich.de (Maximilian Mork)

Nomenclature

Abbrevations

ADMM	Alternating Direction Method of Multipliers
AHU	Air Handling Unit
BLT	Block-lower Triangular
CCA	Concrete Core Activation
COP	Coefficient of Performance
FMI	Functional Mockup Interface
HVAC	Heating, Ventilation and Air Conditioning
illum	Illuminance
KPI	Key Performance Indicator
MAE	Mean Absolute Error
MPC	Model Predictive Control
NLP	Nonlinear Programming
PID	Proportional-Integrative-Differential
RBC	Rule-Based Control
RMSE	Root Mean Square Error
TABS	Thermally Activated Building Systems
VAV	Variable Air Volume

Subscripts

al	Artificial lighting
Conv	Convector
dl	Daylight
inclinationAng	Inclination angle of Venetian blind
posShading	Shading position of Venetian blind
set	Set-point

Indices and sets

$i \in \mathcal{N} := \{1,2,\ldots,\mathrm{N}\}$	Zone of building
$j \in \mathcal{J} := \{1,2,\ldots,\mathrm{J}\}$	MPC iteration
$k \in \mathcal{K} := \{1,2,\ldots,\mathrm{K}\}$	Iteration in distributed approach
$t \in \mathcal{T}$	Time step

Parameters

J	Prediction horizon
K	Maximum number of iterations of distributed approach
N	Number of zones
α	Energy weighting factor
δ	Threshold
θ	Discomfort price
ρ	Penalty parameter

Variables

r	Residual
T	Temperature
u	Control input
ε	Slack variable

λ	Dual variable

1. Introduction

The building sector accounts for approximately 40 % of the final energy consumption and 36 % of all CO2 emissions in the European Union (EU) [1, 2]. Energy goals set by the EU aim at a reduction of greenhouse gas emissions by 2030 by at least 50 % compared with 1990, energy consumption reduction by 2050 by as much as half compared to 2005 and a fully decarbonized building stock by 2050 [2, 3]. HVAC systems are responsible for the major portion of the energy used in buildings [4, 5] which renders them a suitable candidate for increasing building energy efficiency and reducing energy consumption to contribute to the goal of climate-neutrality of Europe by 2050. Apart from building renovations or improvements of the building envelope, building automation systems controlling the building HVAC components suit as an effective approach for substantial energy consumption reduction. Control of HVAC systems, especially for large-scale buildings, is challenging due to time-varying non-linear dynamics, set-points and disturbances and a high amount of interactions [6]. Classical currently implemented control strategies for buildings are Rule-Based Control (RBC) or Proportional-Integrative-Differential (PID) controllers due to their simplicity and low computational requirement [7]. However, they need to be tuned and are not able to consider system and comfort constraints, to handle time-varying systems dynamics or time-delay and to deal with multi-objective cost functions. For large-scale buildings, the rule generalization is very complex due to the thermal and hydraulic coupling between the zones and HVAC components.

Model Predictive Control (MPC) has gained a lot of attention in the context of building control as a promising, powerful control scheme with substantial benefits over conventional controllers [8]. It can predict future disturbances and consider conflicting optimization goals as well as time-varying building dynamics, system and comfort constraints. Building characteristics that are beneficial for use in an MPC are a high thermal mass/ thermal storage, large internal and external heat gains (occupancy, solar radiation) and slow dynamic HVAC system behavior [9]. Apart from this, the demands on comfort (e.g. thermal, indoor air quality, visual) have increased with people in industrialized countries spending on average 90 % of their lifetime in buildings [10].

Implementations of MPC in the form of simulative or practical studies have increased within the last years. Applying the MPC to the operation of a large-cooling system in a university building in Merced, Ma et al. [11] reached savings of 19 % in terms of a coefficient of performance. The application of MPC in a real office building in Prague demonstrated energy consumption savings of 15 to 28 % compared to the reference conventional control based on a heating curve [12]. West et al. [13] applied the MPC on an HVAC system of two office buildings in Australia resulting in an energy reduction of 19 % with similar comfort levels. Similar results are obtained with more than 20 % energy savings in a research laboratory in Illinois [14], more than 20 % primary energy reduction in an office building in Brussels [15] and a primary energy reduction of 17 % for a large-scale simulation in a Swiss office building [16].

When applying MPC to large-scale, multi-zone buildings the optimization problems can become very large and computationally challenging. The computational complexity of the optimization problems further increases due to the inherent nonlinearity in the dynamics and characteristics of the building and HVAC system [17]. With the increase of state and decision variables, the computational complexity of the MPC grows substantially. The time needed for the algorithm to converge to a global optimum increases exponentially with an increase in complexity [18]. This can lead to scalability issues when the large optimization problem cannot be solved at all or in appropriate time, which limits the real-time capability of the MPC implementation. An approach to cope with this challenge is distributed MPC which splits the original central optimization problem into local subproblems. The coordination of the local subproblems can be executed locally by communication between the subproblems or via a global coordinator.

This work is structured as follows. In Section 1.1 a literature research on distributed MPC for large-scale, multi-zone building energy systems is conducted categorizing the research studies into different distributed optimization methods. Section 1.2 outlines the contributions of this work. In Section 2 a multi-zone building model is presented which builds the base for the application of the proposed distributed MPC. Section 3

elaborates the methodology, structure and communication scheme of the distributed MPC approach. In Section 4, the proposed method is applied to a six-room nonlinear Modelica model, compared to a centralized and decentralized reference control and the results are discussed. Finally, a conclusion is drawn and an outlook on further extensions and improvements of the framework is given.

1.1. Background

A distributed MPC addresses the aforementioned challenges for MPC in large-scale, multi-zone buildings and improves the control performance due to several benefits. Computational demand, memory usage and computation time can be reduced by splitting the central problem into subproblems allowing for a distribution of the computation demand. Scalability and real-time capability of the MPC approach are improved. Real-time capability describes the ability to solve the optimization problem by calculating new optimal control inputs within the time of the MPC sampling period which is adjusted to the dynamics of the controlled building. By making use of a distributed MPC the adaptability, extensibility and maintainability of the MPC are enhanced as local subsystems can be replaced, removed or added without changing the remainder of the control system. This is relevant as the replacement of components or renovations/ retrofits of parts of the building are probable within the lifetime of a building. The distributed approach enhances the reliability and stability of the control as subsystems can be easily updated or removed in a plug-n-play approach avoiding an overall control loss. Furthermore, a distributed MPC fits well with the distributed structure of a building (multi-zone, multi-floor composition). The communication overhead and requirements are reduced as large parts of the communication information can be handled locally and are not transmitted to a centralized optimization, which could be prone to communication failures and a corresponding control breakdown. Failures in the local optimizations or communication in one of the subzones do not prevent the overall MPC from operating.

Reviewing the literature for MPC in large-scale, multi-zone buildings, distributed approaches attracted proportionally little attention compared to the number of studies on building MPC, which may be explained by the nonlinear characteristics in building energy systems that complicate convergence guarantees for nonlinear distributed approaches [19]. The distributed MPC approaches in the existing research papers can be classified according to the following criteria:

- Applied mathematical method
- Linearity/ nonlinearity of the controller model
- Cooperative/ uncooperative
- Iterative/ non-iterative
- Consideration/ neglection of thermal (wall/ door) coupling
- Consideration/ neglection of hydraulic HVAC coupling
- Parallel/ sequential computation
- Modeling depth of building envelope and HVAC
- Coordination locally/ via a global coordinator

The dominating applied mathematical methods are:

- (Primal-dual) active-set method
- Benders decomposition
- Dual decomposition

- Information exchange
- Non-iterative lookup tables
- Nash equilibrium
- ADMM

The primal-dual active-set method [20] is based on local identification of active sets (variables at lower or upper bounds) and local updates of dual variables for the inequality constraints based on the active sets. Globally, the non-active primal and dual variables for the equality constraints are calculated setting the inequality inactive dual variables to 0. The iterative, parallel approach is applied to a linear model of an HVAC system with an Air Handling Unit (AHU) for central supply air conditioning in the form of cooling and local Variable Air Volume (VAV) boxes for local reheating/ recooling. It considers thermal coupling as a disturbance.

Moroşan et al. [21] propose a Bender´s decomposition method for distributed MPC of a multi-zone building with central and local zone-individual air conditioning through an AHU. The central control input of the AHU is regarded as the complicating variable. The algorithm consists of solving a global master problem with respect to the global complicating variable and solving the local problems with respect to the local primal and dual variables. The variables of the respective other step are fixed. If the problem does not converge, a new constraint is added to the master problem (called Benders cut). The iterative, linear approach considers thermal and hydraulic coupling and allows for parallel computation.

Dual decomposition is a widespread iterative, cooperative and parallel approach to implement distributed building MPC. It relies on the Lagrangian formulation of the optimization problem, which allows a separation of the optimization problem and ensures the fulfillment of the constraints of the original problem through consistency constraints and updates of dual variables [22]. Ma et al. [23] propose a combination of a dual decomposition and a subgradient method tailored to multi-zone buildings with AHU systems consisting of a central air conditioning as well as locally controlled VAV boxes. The nonlinear model is linearized at each sampling time resulting in a Sequential Quadratic Programming (SQP) problem and considers thermal coupling. Long et al. [24] implement dual decomposition based on a subgradient method in a stochastic MPC for multi-zone buildings with local AHUs. The model is linearized by replacing the bilinear AHU control input term (mass flow multiplied with temperature difference) with a surrogate control input. The approach takes thermal coupling into account and does not consider any hydraulic coupling. Eini and Abdelwahed [25] develop a distributed MPC approach for a multi-zone building equipped with zone heaters with a focus on thermal coupling based on dual decomposition. Thermal coupling is considered through walls and doors. Door coupling is modeled in a simplified form fixing the air exchange between zones through doors to a parameter.

There are further approaches for distributed building MPC that do not rely on a specific class of algorithm for decomposition or distributed optimization but build upon information exchange between (neighboring) subsystems. Putta et al. [26] implement an iterative distributed building MPC approach where the control inputs of sensible cooling of all zones are coupled in the global power consumption. After decoupling the optimization into subsystems, the zone-wise trajectories for the sensible cooling and the states are exchanged between the zones at every iteration until convergence. The distributed parallel, uncooperative approach is applied to a nonlinear, quadratic optimization problem and considers thermal coupling. Scherer et al. [27] propose a distributed approach based on sequential optimizations tailored to sequentially structured subsystems. The subsystems are coupled through a maximum supply water flow and each subsystem introduces a term in its objective modeling the influence on the dynamics of the next downstream subsystems. A subsystem agent receives the residual water flow from its upstream agent, information about the decisions for its downstream neighbors from the last iteration and solves its local optimization. The iterative, sequential and cooperative approach uses a linear controller model and neglects thermal coupling. Radhakrishnan et al. [28] employ a hierarchical-distributed method for multi-zone buildings with central air conditioning which splits the nonconvex optimization problem into three sequential subproblems minimizing the energy consumption of a chiller and a fan. In the first subproblem, an uncooperative distributed nonconvex MPC

minimizes the chiller consumption of all zones (with a fixed chiller coefficient of performance (COP)) based on a linearized model considering the thermal neighbor coupling as a disturbance term. Subproblem 2 and 3 minimize the energy consumption of the chiller (with variable COP) and fan and are constrained by providing the requested minimum cooling energy from subproblem 1. The non-iterative approach is executed in parallel for subproblem 1 and in a sequential, centralized manner for subproblems 2 and 3.

In contrast to the iterative approaches, Baranski et al. [29] propose a sequential, non-iterative approach for a distributed building MPC based on the generation of look-up tables. The concept is tailored to systems with a sequential structure such as in AHUs but can also handle parallel systems at the end of the supply chain. For a predefined grid of combinations of coupling variables, the subsystem optimization problems are optimized via a pattern search algorithm storing the results in three look-up tables (input: combination of coupling variables, output: cost, outflow conditions and decision variables). Beginning with the last subsystem in the supply chain the table is provided to its neighboring upstream subsystem where based on interpolation of the look-up tables, upstream subsystems can estimate the cost their control decision will cause in downstream subsystems. The approach is applied to a nonlinear HVAC system model consisting of two identical rooms equipped with decentralized air handling units and a central heat pump and boiler. The cooperative approach does not consider thermal coupling, focuses on exergy destruction and uses nonlinear Modelica models from a building energy simulation library as simulation models. Based on this work, in [30] multi-layer Perceptron models are fitted by data from Modelica simulations to be used for a Brute Force optimization solver to speed up the subsystem optimizations. Kümpel et al. [31] modify the concept by introducing a coordinator agent sending set-points to the subagents to be more suited to circular connected systems. The subagents create lookup tables where subsystem cost and output variables are calculated based on a simulation for a predefined set of inputs of coupling variables and set-points for the output variables. The look-up tables are sent to the coordinator agent, which minimizes the sum of all subsystems costs and calculates optimal set-points for the coupling output variables for each subagent.

Nash optimization is a further approach used in distributed MPC for multi-zone buildings, which is characterized by an uncooperative, parallel and iterative structure based on information exchange. By solving the subproblems in an uncooperative but iterative way, the subsystems receive updated information for the coupling variables from interconnected subsystems in each iteration and solve their subsystem optimization problems again. If the local optimization results differ less than a fixed threshold between two successive iterations and cannot be improved anymore, the subsystems have converged to the "Nash equilibrium". In contrast to the cooperative approaches, the local cost functions do not include terms considering neighboring or connected agents. Moroşan et al. [32] introduce the Nash optimization method into the field of multi-zone building MPC with a focus on thermal coupling. The neighboring rooms exchange future output trajectories to be able to calculate the inter-zone influences. The approach is applied to a linear model without considering any hydraulic coupling. Similar approaches of exchanging state and output information to consider thermal coupling and reach a Nash equilibrium are used in [33] and [34].

A further common concept for distributed building MPC is Alternating Direction Method of Multipliers (ADMM) [35]. It makes use of the augmented Lagrangian, i.e. the Lagrangian formulation plus an additional quadratic penalty term for increased robustness and better convergence compared to Dual Decomposition. ADMM uses two sets of variables which allows a separation of the objective function. Optimization is done with respect to one variable set with the other one fixed and vice versa (alternating direction). Updates of the dual variables coordinate the fulfillment of the coupling constraints through the variable sets [35]. ADMM is guaranteed to converge for convex problems and only under specific assumptions for nonconvex problems; however, applying ADMM to nonconvex problems performs well on a broad class of nonconvex problems [36, 37, 38, 39]. In the current research of distributed building MPC, ADMM has drawn lots of attention and is generally considered one of the most promising methods for distributed optimization [40]. It is an iterative, cooperative method that is implemented mostly in a parallel computation form. Cai et al. [41] develop an agent-based ADMM distributed MPC approach for multi-zone buildings that are equipped with an AHU. For the subsystems (both individual zones and AHU components), local copies of global variables are introduced and their coincidence is ensured by equality consensus constraints which allow for splitting of the optimization problem. The parallel approach is applied to a case study of a nonlinear multi-zone building model served by a detailed AHU model taking into account thermal coupling. In [42]

a demand agent is added to the ADMM concept which considers a demand charge for the sum of all peak demands. The cooling energy for all subsystems is provided by a central chiller and a fan whose maximum capacity is also considered as a coupling constraint. Local copies are introduced for the subsystems and the linear model consists of three office spaces coupled to local AHUs and a central chiller neglecting thermal coupling. Hou et al. [43] propose a distributed approach based on a Proximal Jacobian ADMM, a modified version of the traditional Gauss-Seidel ADMM especially tailored for parallel computation of a multi-block ADMM. Consensus constraints due to coupling in zone dynamics (thermal coupling) and cost function as well as shared constraints due to shared resources (total mass flow rate from AHU) are introduced using local copies of the coupling variables. The approach is applied to a linear model of a multi-zone building coupled to an AHU in consideration of the bounded total mass flow rate. Lin and Adetola [44] propose a parallel ADMM method for a multi-zone building equipped with an AHU to provide ancillary services to the power grid. The AHU is controlled through the global supply air temperature and local zone-individual airflow rates. The thermal dynamics of the zones (no consideration of inter-zone thermal coupling) and coupled global cost function are decoupled concerning the central AHU by introducing copies for the supply air temperature for each zone, the airflow rates of each zone and a sharing constraint for the sum of the zone flow rates. Yang et al. [45] employ a parallel, modified version of the ADMM, the Accelerated Distributed Augmented Lagrangian (ADAL), for a multi-zone building equipped with a central AHU and local VAV boxes. An additional virtual agent is introduced considering the maximum bound of the sum of local airflow rates. The approach considers thermal coupling and is implemented on a linearized surrogate model of the multi-zone building.

Hydraulic coupling between different zones in buildings can be induced by thermally activated building systems (TABS) which is a heating and cooling system allowing to use the thermal mass of the building as thermal storage. Water pipes embedded in the center of the concrete provide the heating or cooling energy and transfer it to the inert concrete of floors or ceilings, which transfer the heating or cooling energy to the room. TABS distributors providing the heating or cooling energy to the rooms through pipe systems are not controlled room-wise due to the slow dynamics and inertia and couple several rooms together [46]. To consider hydraulic TABS coupling Killian et al. [47] develop an uncooperative distributed MPC for a multi-zone building where all rooms are equipped with local fan coils and coupled to central TABS. Based on sequential, iterative information exchange the local fan coil MPCs and the central TABS MPC calculate overall control inputs considering the control decision of the respective other systems as disturbances. Thermal coupling is neglected in the approach.

1.2. Contribution

The major novelty of this work consists in the implementation of a distributed gradient-based MPC concept for multi-zone buildings based on Modelica controller models. In this manner, the advantages of the Modelica language and its extensive building simulation libraries are extended to the use in large-scale, multi-zone buildings based on a gradient-based distributed MPC. In the majority of the cited research studies, simulation and controller models are built in a simplified form regarding the building envelope (walls, windows and doors), thermal transfer phenomena (convection, radiation and conduction) and in particular the modeling of the HVAC system. In the proposed distributed MPC in this work, the building envelope as well as the HVAC components are modeled in a detailed way with respect to relevant physical phenomena and dynamics. The distributed MPC concept is applied to local nonconvex optimization problems based on nonlinear controller models, which are implemented sparsely in literature. In the distributed optimization method an uncooperative and a cooperative approach are combined addressing thermal and hydraulic coupling at the same time. The uncooperative part accounts for the thermal coupling between the zones and builds upon the Nash optimization. The cooperative part considers the hydraulic coupling of the zones through a central, shared HVAC system and is implemented with an approach based on ADMM. Making use of the consensus ADMM implementation the approach is tailored to controlling the thermal mass of a building through TABS, and thereby exploiting passive storage capacities of buildings, which are essential to integrate buildings in future global energy systems. The overall distributed method is iterative and allows for parallel computation. It is structured in a plug-n-play fashion for easy extensibility and adaptability based on an automated central coordinator.

With regard to the thermal coupling, detailed models of thermal coupling through doors are implemented which are not integrated in the distributed building MPC literature as far, apart from simplified door modeling approaches [25]. As shown in the course of this paper, the impact of open door coupling is substantial compared to wall coupling and thus, should be taken into account. To keep the computational demand of the distributed MPC low, a data-driven modeling approach is used which is fitted and validated with data from simulations including a detailed door model from a Modelica building simulation library. The data-driven model calculates the air exchange between two door-coupled rooms based on the room air temperature difference.

Finally, a block-lower triangular (BLT) decomposition scheme is employed to reduce the number of algebraic variables in the subproblems, which tend to be high for building energy systems models. The overall distributed MPC approach is applied to a detailed nonlinear six-room-building model, which is implemented in Modelica and features both thermal and hydraulic coupling.

In summary, the innovations of this paper within the scope of distributed MPC in multi-zone buildings are:

- Distributed gradient-based MPC for multi-zone buildings based on Modelica controller models
- Simultaneous consideration of thermal and hydraulic coupling using Nash equilibrium and ADMM
- Detailed modeling of the thermal coupling through doors (based on a data-driven modeling approach)
- Application of distributed MPC on nonlinear controller models with detailed HVAC components considering both thermal and hydraulic TABS coupling

2. Modeling

The methodology for the distributed approach is inspired by the case study model but is also applicable to more general coupling forms. The multi-zone building model is implemented in the form of a nonlinear white-box model in the modeling language Modelica [48]. When implementing MPC in buildings the modeling part accounts for the major portion of project time and costs and therefore plays an essential role in the success of an MPC implementation [12]. Modelica suits the use in MPC for several reasons. It is an open-source, equation-based, acausal and object-oriented modeling language with a graphical interface to connect components [49]. These characteristics point out the flexibility and modularity of Modelica which is crucial taking into consideration that every building is unique. In common projects, extensive open-source Modelica simulation libraries for building energy systems have been developed by experts [50]. Modelica supports the Functional Mockup Interface (FMI) standard that allows the model exchange or co-simulation with other simulation programs and suits both simulation and (gradient-based) optimization due to the language extension Optimica [51].

The base for building the controller and simulation models in this work is the open-source Modelica simulation library AixLib [52]. The AixLib provides models of HVAC systems as well as high and reduced-order building models. An optimization library is developed by adapting the AixLib models for compatibility with the used optimization framework JModelica.org [51] and the solver IPOPT [53]. JModelica.org is used for the gradient-based optimization of Modelica models and is equipped with an interface to IPOPT, which is an open-source nonlinear solver able to solve large-scale nonlinear problems. More details regarding the necessary modifications of the AixLib models can be found in [54]. Modified AixLib models are validated trough simulations comparing the results with the ones of the original models.

The building model structure is shown in Fig. 1 and consists of six rooms that are coupled thermally (via walls and inner doors; outer doors are not modeled here) and hydraulically. High-order room models are chosen to retain the neighboring coupling structure among the rooms. All room models are equipped with a dynamic air model (*MixingVolume*), external and inner walls, windows with models for external Venetian blinds for active solar shading (for more information regarding the Venetian blind models see [54]), simplified pumps, a convector and are coupled to a central, shared TABS implemented as Concrete Core Activation (CCA) in the floor. The central CCA is controlled via one shared control input for the overall CCA zone

regulating the supply water mass flow. Pumps supply both the CCA and the convector with supply water flows at fixed temperatures. Thermal transfer is taken into account in the form of convection, conduction and radiation (longwave radiation exchange inside the room modeled based on the AixLib "two star" room model). An occupancy model calculates human heat emissions according to office-typical schedules (8 a.m.–12 p.m. and 1–6 p.m.). Weather data from an AixLib resource file for San Francisco in January 1999 is input to the model and comprises a heating period. To focus on the functionality and performance of the distributed MPC approach, no model mismatch (controller model identical to simulation model) and a perfect forecast of the disturbances are assumed.

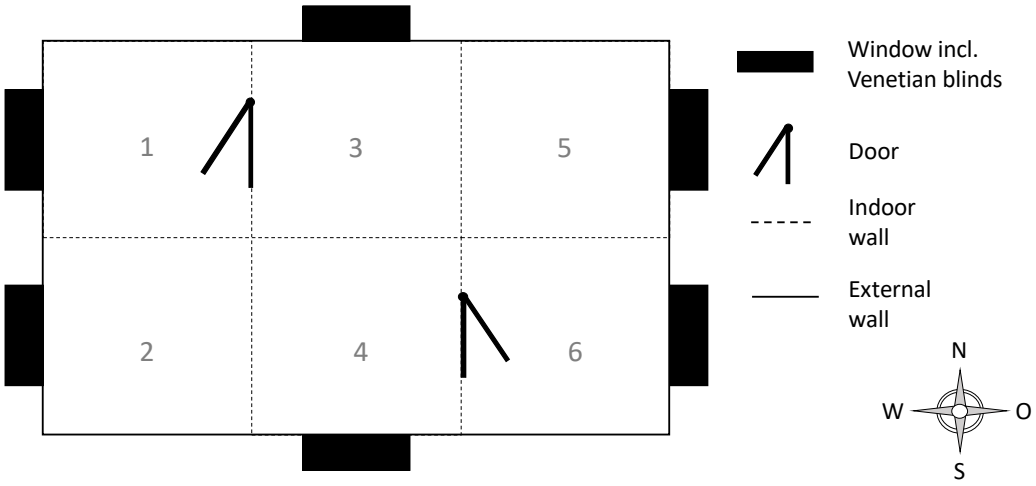

Figure 1: Structure of the Modelica six-room-building-model including thermal coupling components

Control inputs of the sub-models are the local water mass flows to the convectors, the shared, central global water mass flow to the CCA and the vertical position and inclination angle of the external Venetian blinds accounting for both thermal and visual comfort (minimum illuminance of 500 lux in occupied times). Artificial lighting is not modeled explicitly and the artificial lighting power consumption is assumed to vary linearly with the required artificial illuminance. An individual room overview including the components and control inputs is shown in Fig. 2. To further increase energy efficiency and take advantage of the predictive control concept in the scenario of an office building, a night set-back is implemented for the temperature range which implicates that during unoccupied (night) times the thermal comfort ranges are wider than for occupied times (occupied times: 293 - 295.5 K, unoccupied times: 292 K - 296.5).

The physics-based, white-box controller model is nonlinear due to the characteristic nonlinearities inherent in the thermal transfer phenomena (radiation, convection) and the HVAC systems leading to a nonlinear programming (NLP) problem. Compared to linear simplified models, nonlinear models reproduce the real building behavior more precisely over the whole operation range and enable a higher potential of MPC savings closer to the theoretical performance bound. Apart from this, they allow more flexibility in formulating the model equations, constraints and cost function [17]. A further advantage of nonlinear building MPC is that models can be directly configured based on (adapted) building simulation libraries. The efforts for pre- and postprocessing, variable mapping and linearization are reduced and optimization with respect to the control inputs that are implemented in the real system is enabled. Especially for the use in MPC a model of high accuracy is essential, as an MPC tends to operate the room temperatures near the bounds to save energy where an inaccurate model would increase the risk of comfort violations. The use of physics-based nonlinear models comes at the cost of higher computational demand; however, due to current improvements of optimization algorithms and solvers as well as developments in server and cloud computing the computational power is increasing exponentially [7]. In white-box models, the parameters and (input) variables preserve their physical meaning and have a geometrical equivalent inside the real building in contrast to gen-

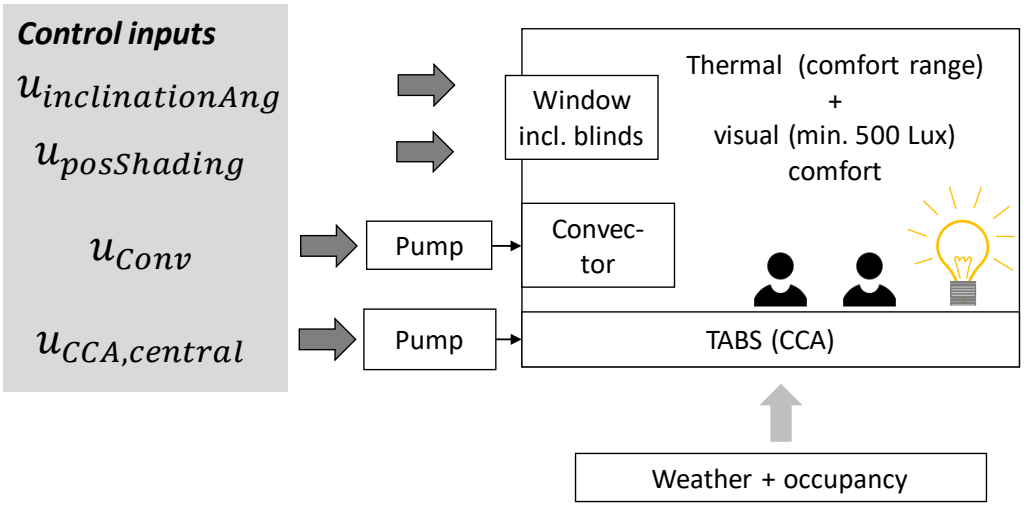

Figure 2: Room structure including components and control inputs

eral grey-box and black-box approaches [55], which ensures their explicit location, improved comprehension of the system behavior and fault detection. The distributed optimization in the proposed approach alleviates using local high-accuracy models compared to a centralized variant as the overall model complexity is reduced in the spatial dimension by splitting the problem.

According to Fig. 1, the rooms are coupled thermally via inner walls and inner doors. As shown in Fig. 3 and a simulative study of thermal coupling between rooms of different temperatures (door area of 1,9 m^2 and wall area between the coupled rooms of 15 m^2), thermal coupling induced by open doors can cause heat flows that are larger than the ones induced by wall coupling. To take the door coupling into account a data-driven model is created. The data is generated in a simulation of two rooms coupled through an accurate AixLib door simulation model which calculates the bi-directional airflow through a door, is discretized along the height coordinate and which has either an open or closed opening state. To analyze a large range of (both positive and negative) temperature differences between the rooms, artificial heat gains are added to the rooms. The data-driven model is based on polynomial regression using scikit-learn [56] and calculates the exchanged volume airflow between the rooms as a function of the room temperature difference. Derived from the simulation results, the air exchange for a closed door can be considered negligible and is set to zero. The regression function is of order 4, only includes coefficients of even order and thus is symmetrical. By using the data-driven door model the computation times can be significantly reduced compared to using the original simulation model in the MPC . The data-driven model is validated by comparing the calculated exchanged enthalpy flow rates between the rooms with the results from the original door simulation model which is shown in Fig. 4. For temperature differences between -2 and 2 K where most of the thermal coupling takes place, the results are visually and numerically very close to the original results. The Mean Absolute Error (MAE) is 8.4 W, the Root Mean Square Error (RMSE) is 10.9 W. In this work, the door opening state is considered predictable and assumed to be open when the rooms are occupied. In a practical implementation, the opening status could be predicted based on historical data of the user behavior using door sensors.

3. Methodology

In this work, a gradient-based distributed MPC approach for multi-zone building models based on Modelica controller models is proposed. It simultaneously considers thermal coupling through walls and data-driven door models as well as hydraulic coupling induced by a central HVAC system. In the focused case study, the central HVAC consists of TABS implemented as CCA in the floor. The functionality of CCA builds upon

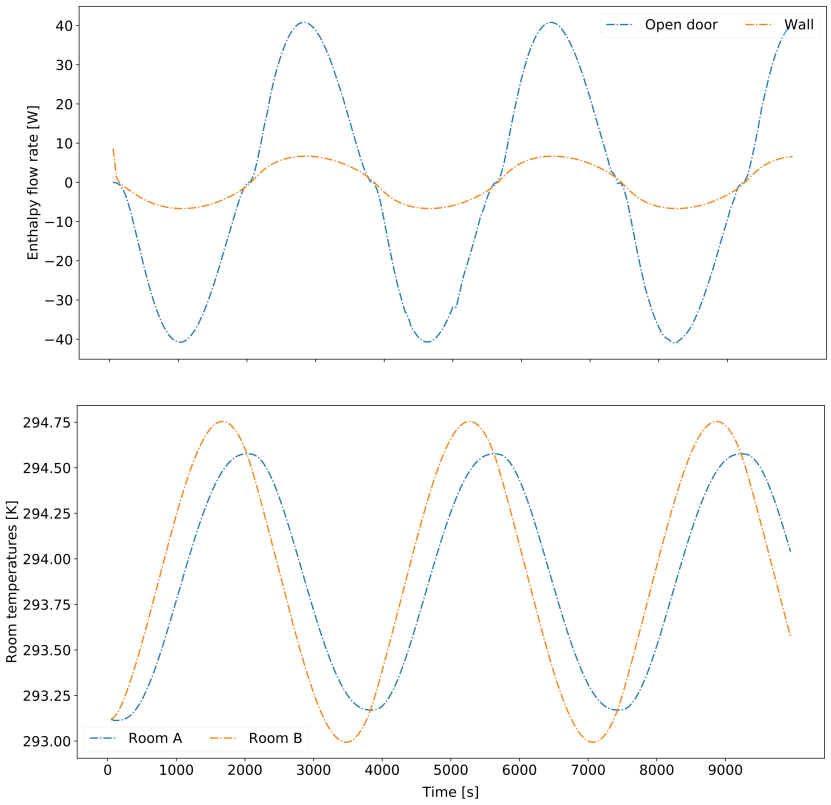

Figure 3: Comparative study of thermal coupling through an open door and wall for a simulation of two coupled rooms with different room temperatures

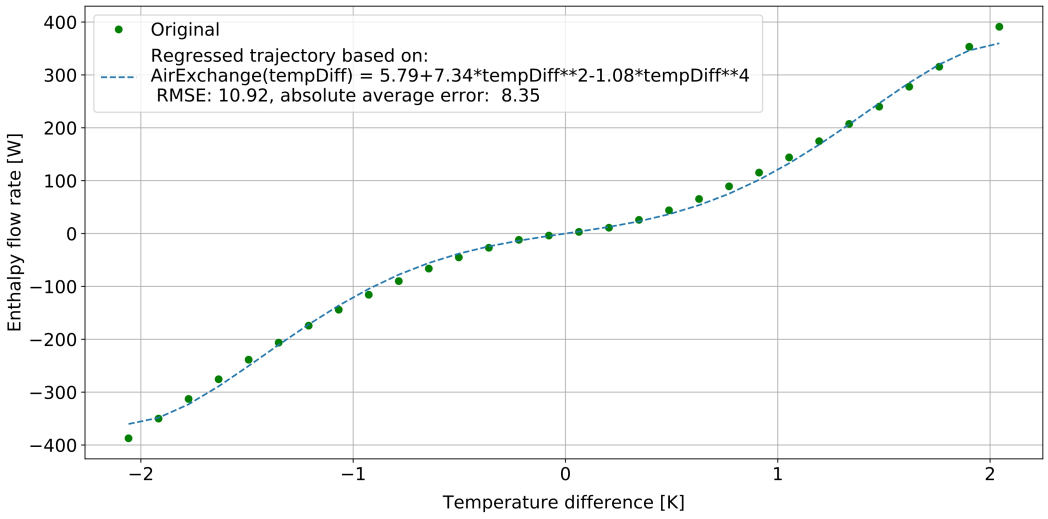

Figure 4: Comparison of the regressed trajectory for the exchanged enthalpy flow and the simulated trajectory of the original door model

the activation of the thermal mass of the building in the form of the concrete. The activation allows for the use of the building mass with potential high inertia as passive storage to shift the time of energy supply and demand which is a valuable characteristic in the context of volatile renewable energy supply. Due to the high time delay and inertia, the use of MPC as an anticipatory control concept is beneficial compared to conventional control strategies. Through its high thermal capacity, CCA is well suited for covering the building heating/ cooling base load while more dynamic and reactive actors (in this case study the convectors) provide the peak load. Making use of the radiative heating concept in CCA (in contrast to convective concepts) low-temperature heating (or high-temperature cooling) energy can be integrated which increases energy efficiency and enables the use of waste heat on low-temperature levels from data centers. Due to its inertia and slow dynamics, one TABS/ CCA coil generally provides several rooms of similar thermal properties and orientation (e.g. division a building floor into a north and south zone) [46]. Therefore, it introduces strong coupling between the rooms of the same TABS control loop. It is assumed here that the inlet water temperatures for every CCA room section in one CCA coupled zone differ in a negligible way due to a uniform arrangement of the CCA coils in parallel to the rooms. In the following, the supply water temperatures are considered identical.

The two inter-zone coupling forms are integrated based on two different mathematical methods. The thermal coupling is considered through an uncooperative Nash equilibrium approach whereas the hydraulic coupling is incorporated through a cooperative consensus ADMM approach. The uncooperative Nash optimization considers the room temperatures of neighboring zones as known disturbances and is chosen for thermal coupling as it is a distributed optimization method with low computational demand. This reduces the complexity of the distributed method for large-scale buildings. Apart from this, the temperatures for example in office buildings are generally in similar ranges due to similar work and occupancy schedules and heat gains/ losses are generally dominated by internal (e.g. occupancy) or external (e.g. window openings, transmission of solar radiation) heat gains. In addition, the MPC tends to operate the rooms at similar comfort bounds for energy efficiency reasons (lower temperature bound in heating periods, higher temperature bound in cooling periods). Nevertheless, thermal coupling plays an essential role as due to the operation near the comfort bounds unconsidered thermal exchanges between rooms can cause discomfort.

The cooperative consensus ADMM is chosen for the hydraulic coupling as the coupling variables in the form of the local control inputs can differ significantly and the consensus constraint of one central shared control input can only be ensured with a cooperative approach. As stated in Section 1.1, ADMM is regarded as one of the most promising distributed optimization approaches. Both applied approaches are iterative and allow for a computation of the local subproblems in parallel. A global coordination scheme monitors the progress of both approaches and coordinates the subproblems by updating information.

For the thermal coupling (here coupling of the local state variables), the air temperatures of neighboring rooms that influence the dynamics of a subsystem via wall or door coupling are considered as known disturbances. After every optimization iteration, the locally calculated trajectories for the local room temperatures are sent to the coordinator, which then sends them to all neighboring subsystems that are influenced by the corresponding zone, and the local optimizations are repeated. The local optimizations iteratively reach the Nash equilibrium if, for all local subsystems $i \in \mathcal{N}$ and averaged over the MPC horizon $\mathcal{J}$, the absolute deviation of the local room temperatures trajectories between two consecutive distributed iterations $k+1$ and k does not differ more than a prefixed Nash threshold δ_{Nash}:

$$r_{\mathrm{Nash},i} = \frac{1}{|\mathcal{J}|} \sum_{j \in \mathcal{J}} |T^{k+1}_{\mathrm{Air},i,j} - T^{k}_{\mathrm{Air},i,j}| < \delta_{\mathrm{Nash}} \tag{1}$$

The hydraulic coupling (here coupling of the local control inputs) induced by the central CCA is incorporated by a consensus ADMM approach. To decompose the optimization problem coupled through the central, shared CCA control input (here represented by the CCA supply water mass flow), for every subsystem $i \in \mathcal{N}$ a local copy $u_{\mathrm{CCA,local},i}$ of the global CCA control input $u_{\mathrm{CCA,global}}$ is created. Terms ensuring the consensus of the local copies and the global CCA control input are added to the cost functions of the local subsystems and the coordinator (see Eq. 2 and 10). In the case study model, the local cost

functions in Eq. 2 solve their local subproblems minimizing energy consumption of the convector, CCA and artificial lighting and discomfort (quadratic penalization term for temperatures outside the comfort range through the introduction of slack variables $\underline{\varepsilon}_i$ and $\bar{\varepsilon}_i$) in consideration of the ADMM terms, constraints in Eq. 3 - 9 and the model dynamics. Amongst other control inputs, at iteration $k+1$ of the distributed approach the local CCA control inputs $u^{k+1}_{\mathrm{CCA,local},i}$ are obtained.

$$
\begin{aligned}
&\{u_{\mathrm{Conv},i}, u_{\mathrm{CCA,local},i}, u_{\mathrm{al},i}, u_{\mathrm{posShading},i}, u_{\mathrm{inclinationAng},i}, \underline{\varepsilon}_i, \bar{\varepsilon}_i\}^{k+1} \\
&\quad = argmin_{u_{\mathrm{Conv},i}, u_{\mathrm{CCA,local},i}, u_{\mathrm{al},i}, u_{\mathrm{posShading},i}, u_{\mathrm{inclinationAng},i}, \underline{\varepsilon}_i, \bar{\varepsilon}_i} \\
&\quad [\alpha_{\mathrm{Conv}} * u_{\mathrm{Conv},i} * (T_{\mathrm{supply,Conv},i} - T_{\mathrm{return,Conv},i}) + \\
&\quad \alpha_{\mathrm{CCA}} * u_{\mathrm{CCA,local},i} * (T_{\mathrm{supply,CCA},i} - T_{\mathrm{return,CCA},i}) + \\
&\quad \alpha_{\mathrm{Light}} * u_{\mathrm{al},i} + \theta * ({\underline{\varepsilon}_i}^2 + \bar{\varepsilon}_i^2) + \lambda^k_{\mathrm{Dual,CCA},i} * (u_{\mathrm{CCA,local},i} - u^k_{\mathrm{CCA,global}}) + \\
&\quad \frac{\rho}{2} * (u_{\mathrm{CCA,local},i} - u^k_{\mathrm{CCA,global}})^2]
\end{aligned}
\tag{2}
$$

subject to

$$\underline{T}_{\mathrm{room,air},i} - \underline{\varepsilon}_i \leq T_{\mathrm{room,air},i} \leq \bar{T}_{\mathrm{room,air},i} - \bar{\varepsilon}_i \tag{3}$$

$$\underline{\varepsilon}_i, \bar{\varepsilon}_i \geq 0 \tag{4}$$

$$illum_{\mathrm{dl},i} + illum_{\mathrm{al},i} = illum_{\mathrm{set},i} \tag{5}$$

$$0 \leq u_{\mathrm{Conv},i} \leq u_{\mathrm{Conv,max}} \tag{6}$$

$$0 \leq u_{\mathrm{CCA,local},i} \leq u_{\mathrm{CCA,global,max}} \tag{7}$$

$$0 \leq u_{\mathrm{posShading},i} \leq u_{\mathrm{posShading,max}} \tag{8}$$

$$0 \leq u_{\mathrm{inclinationAng},i} \leq u_{\mathrm{inclinationAng,max}} \tag{9}$$

In these formulations, $u_{\mathrm{Conv},i}$,$u_{\mathrm{CCA,local},i}$,$u_{\mathrm{al},i}$,$u_{\mathrm{posShading},i}$ and $u_{\mathrm{inclinationAng},i}$ are the local control inputs of convector and CCA supply water mass flow, artificial lighting (in the form of the artificial illuminance), shading position and inclination angle. $T_{\mathrm{room,air},i}$ is the room air temperature, $\underline{T}_{\mathrm{room,air},i}$ and $\bar{T}_{\mathrm{room,air},i}$ are the lower and upper comfort temperature bounds, $\underline{\varepsilon}_i$ and $\bar{\varepsilon}_i$ are slack variables, softening the temperature constraint and quantifying temperatures outside the comfort range. $T_{\mathrm{supply,Conv},i}$, $T_{\mathrm{return,Conv},i}$, $T_{\mathrm{supply,CCA},i}$ and $T_{\mathrm{return,CCA},i}$ are the supply and return water temperature of the convector and CCA. α_{Conv} and α_{CCA} are energy weighting factors for the convector and CCA including the heat capacity of water, α_{Light} a weighting factor for the energy consumption of artificial lighting and θ a factor penalizing room temperatures outside the comfort range. $illum_{\mathrm{dl},i}$ is the daylight, $illum_{\mathrm{al},i}$ the artificial light and $illum_{\mathrm{set},i}$ the set-point illuminance. $u^k_{\mathrm{CCA,global}}$ is the global CCA control input from the previous iteration k calculated by the global coordinator, $\lambda^k_{\mathrm{Dual,CCA},i}$ are the dual variables from the previous iteration k and ρ is the penalty parameter. Eq. 6 - 9 contain the minimum and maximum bounds for the control inputs with $u_{\mathrm{posShading},i} \in [0, 1]$ (0: fully opened, 1: closed) and $u_{\mathrm{inclinationAng},i} \in [0°, 90°]$ (0°: fully opened, 90°: closed).

Based on the new calculated trajectories for the local CCA control inputs $u^{k+1}_{\mathrm{CCA,local},i}$, the global coordination scheme calculates the global CCA control input in Eq. 10 and then updates the dual variables (Lagrangian multipliers) for every zone based on the fulfillment of the corresponding consensus constraint ensuring consistency between the local and the global CCA control variables (Eq. 11).

$$
\begin{aligned}
{u_{\mathrm{CCA,global}}}^{k+1} = argmin_{u_{\mathrm{CCA,global}}} [&\sum_{i \in \mathcal{N}} \lambda^k_{\mathrm{Dual,CCA},i} * (u^{k+1}_{\mathrm{CCA,local},i} \\
&- u_{\mathrm{CCA,global}}) + \frac{\rho}{2} * (u^{k+1}_{\mathrm{CCA,local},i} - u_{\mathrm{CCA,global}})^2]
\end{aligned}
\tag{10}
$$

$$\lambda^{k+1}_{\mathrm{Dual,CCA},i} = \lambda^k_{\mathrm{Dual,CCA},i} + \rho * (u^{k+1}_{\mathrm{CCA,local},i} - u^{k+1}_{\mathrm{CCA,global}}) \tag{11}$$

The ADMM penalty parameter ρ appearing in Eq. 2, 10 and 11 is set by the user. A higher penalty parameter implicates a higher weight on the fulfillment of the consistency constraint compared to the energy consumption minimization and vice versa. Here, a two-block Gauss-Seidel ADMM is used where the local optimizations are calculated in parallel and are followed by the global optimization and Lagrangian multiplier update. Compared to the local optimizations in Eq. 2, the computation time of the global calculation in Eq. 10 can be considered negligible. As a global coordinator is used, the approach is not completely distributed but it could be adapted with regards to this. The ADMM applies both a primal and dual residual criterion as a condition for terminating the ADMM iterations (Eq. 12 and 13, based on [35]):

The primal residual for iteration $k+1$ for one zone $i \in \mathcal{N}$ is calculated through:

$$r_{\text{ADMM,primal},i} = \frac{1}{|\mathcal{J}|} \sum_{j \in \mathcal{J}} |u^{k+1}_{\text{CCA,local},i,j} - u^{k+1}_{\text{CCA,global},j}| < \delta_{\text{ADMM,primal}} \tag{12}$$

The dual ADMM residual for iteration $k+1$ is calculated through:

$$r_{\text{ADMM,dual}} = \frac{1}{|\mathcal{J}|} \sum_{j \in \mathcal{J}} |u^{k+1}_{\text{CCA,global},j} - u^{k}_{\text{CCA,global},j}| < \delta_{\text{ADMM,dual}} \tag{13}$$

If both the Nash optimization and the ADMM residuals fall below their corresponding termination criteria for all subsystems the MPC proceeds to the next MPC sampling step $j+1$. Additionally, in every MPC step j, a maximum number of iterations K is set as a termination criterion for the distributed approach. The overall distributed MPC approach based on ADMM and Nash optimization is shown in Algorithm 1.

Algorithm 1: Proposed distributed MPC approach based on ADMM and Nash optimization

Initialization: choose $\rho > 0$, t_{sampling}, set $\lambda^0_{\text{Dual,CCA},i} = 0$, $u^0_{\text{CCA,global}} = 0$; $j \leftarrow 1$; $k \leftarrow 1$; $\mathcal{N}$:={1,. . . ,N}; $t_{\text{simulation,start}} = 0$; $t_{\text{simulation,end}} = t_{\text{sampling}}$
for $j \in \{1,\ldots,\text{J}\}$:
    for $k \in \{1,\ldots,\text{K}\}$:
        For all zones $i \in \mathcal{N}$ in parallel:
            Obtain $u^k_{\text{CCA,local},i}$ minimizing local cost functions according to Eq. 2.
            Send $u^k_{\text{CCA,local},i}$ and local room temperature trajectories to coordinator.
        Coordinator: Obtain $u^k_{\text{CCA,global}}$ minimizing global cost function according to Eq. 10.
        Coordinator: Update dual variables $\lambda^k_{\text{Dual,CCA},i}$ for all $i \in \mathcal{N}$ according to Eq. 11. Send trajectories for $u^k_{\text{CCA,global}}$, $\lambda^k_{\text{Dual,CCA},i}$ and neighboring room temperatures to the subsystems.
        If Nash and ADMM termination conditions are fulfilled according to Eq. 1, 12, 13 or $k = \text{K}$:
            Exit the inner loop and go to Step 10.
        else:
            $k \leftarrow k+1$
            Go to Step 4.
    Local subsystems send control inputs $u^k_{\text{CCA,local},i}$ to the simulation. Compute average CCA control input.
    Simulate for $t = [t_{\text{simulation,start}}, t_{\text{simulation,end}}]$.
    $t_{\text{simulation,start}} \leftarrow t_{\text{simulation,start}} + t_{\text{sampling}}$; $t_{\text{simulation,end}} \leftarrow t_{\text{simulation,end}} + t_{\text{sampling}}$
    Send simulation results to local subsystems to update initial optimization states.

14: If $j = \mathrm{J}$:
Exit outer loop.
15: else:
$j \leftarrow j + 1$ and go to Step 3.

The communication structure is summarized in Fig. 5. In every iteration of the overall distributed method, the local subsystems optimize their subproblems, send the calculated trajectories for their CCA control inputs and the room temperature to the global coordinator. The local optimization results of the respective previous optimization serve as initial guesses to "warm start" a new optimization which is essential for a nonconvex ADMM. Based on the exchanged information the global coordinator optimizes the global cost function calculating new trajectories for the global CCA control input and then updates the dual variables ensuring the consensus constraints between the global and local copies for the CCA input. The coordinator calculates the residuals for the ADMM and Nash optimization and checks if the distributed method has converged under the user-specified thresholds for both ADMM and Nash optimization. It sends the trajectories for the air temperatures, global CCA control inputs, updated dual variables and the iteration convergence status to the local subsystems, which then continue their calculations based on the iteration convergence status. The room temperature trajectories are only sent to the subsystems that are influenced by the corresponding subsystem, i.e. the neighbor systems. If the termination criteria for both ADMM and Nash optimization are fulfilled, the local subsystems send all control inputs calculated in the last iteration to the global coordinator where the local CCA control inputs are converted into one shared averaged value and the simulation on the coupled building model is run for one MPC sampling step. The simulation results after the sampling step are then sent to subsystems to update the optimization states for the next optimization at the next MPC iteration and the MPC iteration counter is increased. If the termination conditions of the distributed MPC are not fulfilled and the maximum number of distributed iterations is not reached, the iteration counter of the internal distributed method is increased and the subsystems solve the subproblems again based on the new information sent by the coordinator.

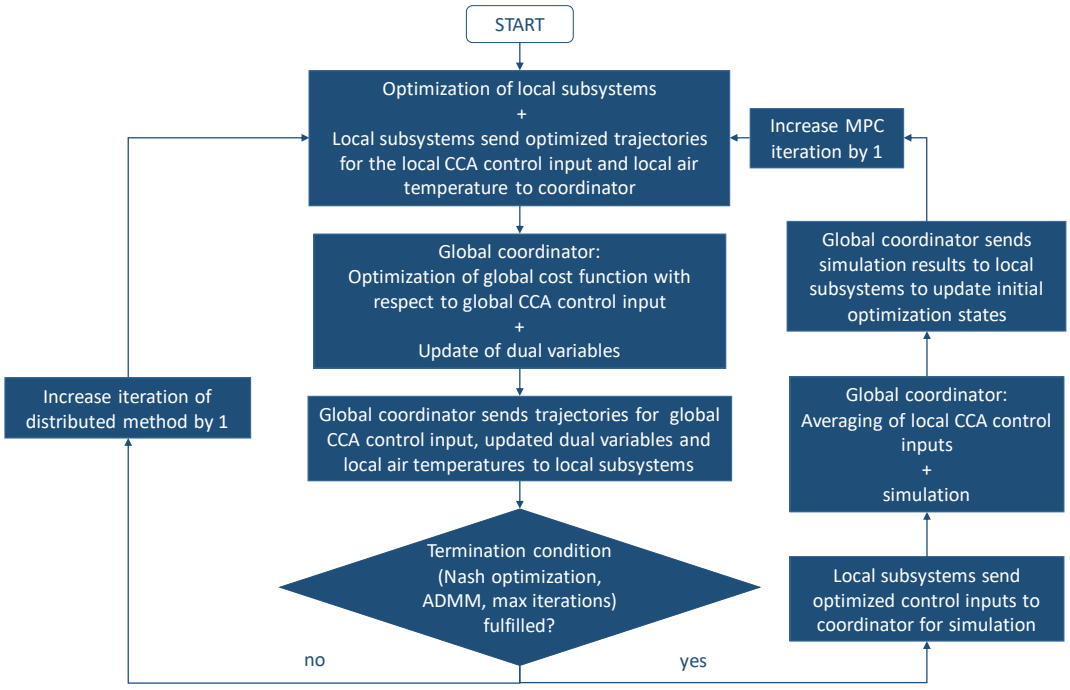

Figure 5: Overall communication structure of the distributed MPC

The multi-zone building model is decomposed zone-wise. To simplify the modeling in Modelica and keep it as modular as possible half-wall structures are used for the inner walls to couple zones together in a straightforward way. To take the thermal coupling through walls into account, in the local controller model the second half of an inner wall of the neighboring room is added in combination with the variable temperature boundary condition component ("PrescribedTemperature") of the Modelica library and the neighbor temperature trajectories sent from the coordinator as input. For considering the thermal coupling through doors the data-driven door models based on the regression functions from Section 2 are integrated calculating the air exchange and enthalpy flow rate based on the air temperature difference between two rooms and the opening state. The general modeling is structured in a manner to easily add further rooms and wall/ door coupling (plug-n-play approach). The zone models used for the coupled global simulation build the base for creating the distributed controller models making use of the Modelica "extend" function, which avoids code duplication and model inconsistencies. Dimensioning, orientations of the internal and external walls and windows including Venetian blinds are set in the Python framework in JModelica.org to keep the framework as automatable as possible. The assignment of neighbors to every room takes place in Python as well. Currently, the adding of zone models and the neighbor assignment is done manually but an automatic building configuration in Python based on room templates is planned. The remainder of the framework is already automated to such a degree as the local subsystems and the global coordinator automatically communicate the relevant coupling variables based on the specified neighbor configuration. For every local controller, an Optimica .mop file is created based on the Modelica (.mo) file to provide further optimization-characteristic information such as the cost function and constraints. The overall distributed MPC framework is written in Python based on JModelica.org. The complete toolchain is shown in Fig. 6.

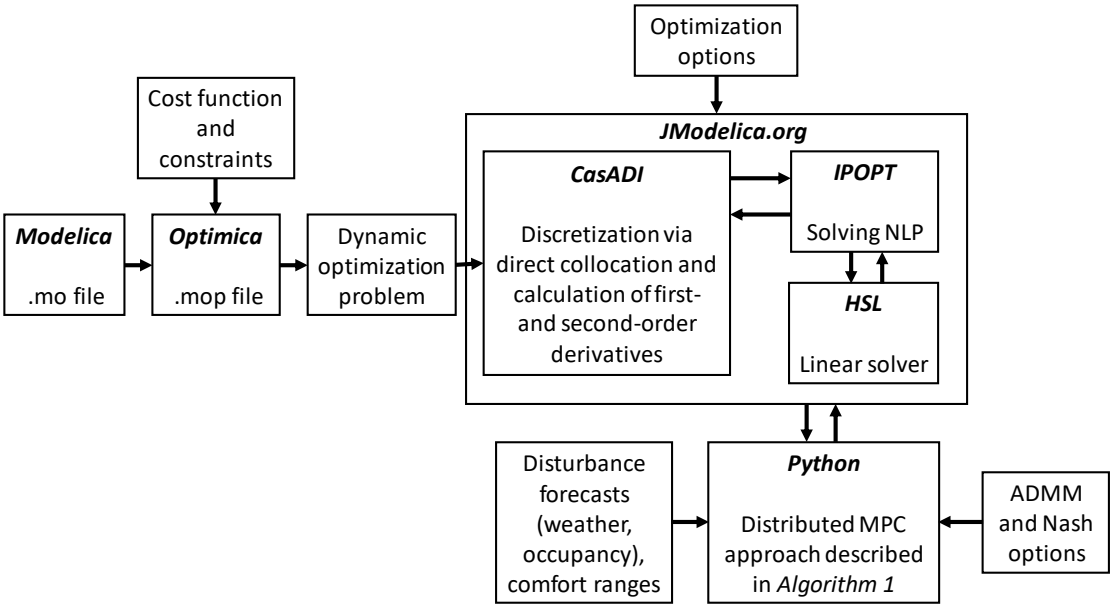

Figure 6: Overview over toolchain for implementation of the distributed MPC approach

To further reduce computation time and controller model complexity and alleviate the use of high-accuracy models, a block-lower-triangular (BLT) decomposition method based on the JModelica.org framework is employed [57]. By solving some of the algebraic equations of the differential-algebraic equations (DAE) in a preprocessing step, the number of algebraic variables in the optimization problems, which tends to be high for the focused energy systems (significantly higher than the number of state variables), can be considerably reduced. The framework includes the features of block-triangular ordering, tearing and sparsity preservation. It has to be noted that not all algebraic variables can be marked as eliminable as some are essential for reproducing the system dynamics and preserving system stability. Conducting large-scale sim-

ulations, these variables are derived and marked as non-eliminable. Further, algebraic variables appearing in constraints or the cost function are excluded from being eliminated.

4. Results and discussion

In a simulative case study, the proposed distributed MPC approach is applied to the nonlinear building model described in Section 2 containing detailed component models for the building envelope and HVAC. To validate the functionality of the approach in a scenario where thermal and hydraulic coupling have a large impact on the system behavior, occupancy heat gains of different dimensions are generated in the differently oriented rooms. In this way, temperature differences are created which induce heat flows between the rooms. In a decentralized MPC neglecting any coupling, the local subsystem controllers would control their corresponding CCA control inputs different from each other based on the respective heat gains in the room. This would violate the constraint of a global, shared CCA control input. Therefore, this scenario is suitable to analyze how well the approach integrates thermal and hydraulic coupling.

To compare the performance of the method against alternative control methods, additional MPC variants in a centralized and a decentralized form are applied. The centralized concept consists of one central controller that calculates the large-scale optimization problem considering all coupling forms. It intrinsically accounts for the thermal coupling and is constrained by one shared global CCA control input which is applied to every room. The decentralized variant consists of local controllers neglecting any thermal and hydraulic coupling. In the non-centralized approaches (distributed and decentralized variant), the shared CCA control input applied to the simulation model is calculated by averaging all optimized control inputs from the local optimizations. The control quality is quantified in terms of the following Key Performance Indicators (KPIs): Energy consumption (weighted sum of CCA, convector and lighting, in kJ), thermal discomfort (quantifying the amount of Kelvin hours during which the local room temperatures are outside the comfort range, in Kh) and computation time/ computational time ratio. Computation time comprises the time used for the total MPC. The computational time ratio quantifies the relation of the computation time to the sampling time (time span during which the building is controlled). If the ratio is < 1, the control strategy is real-time capable. All control strategies are executed in JModelica.org 2.14 including PyFMI for the simulation, IPOPT 3.13.1 and the linear HSL solver ma27 [58]. For solving the MPC problems, an OpenStack instance based on a Linux machine, Ubuntu 18.04, 8 VCPUs and 32 GB RAM is used. For the discretization via collocation, 96 collocation elements with 2 collocation points are chosen. All MPCs have a prediction horizon of 24 h and a sampling period t_{sampling} of 15 min. The simulation horizon (sampling time) is 5 days (=120 h) and starts at 8 a.m. The penalty parameter ρ is set to 10^2, the primal ADMM threshold $\delta_{\text{ADMM,primal}}$ to 0.01, the Nash threshold δ_{Nash} and dual ADMM threshold $\delta_{\text{ADMM,dual}}$ to 0.2. The maximum number of distributed iterations K is set to 7.

In Fig. 7 the simulation results of the distributed MPC approach are shown. The "Outdoor temperature", "Solar radiation" and "Occupancy" subplot depict the different disturbances affecting the system behavior. The outdoor temperatures during hours 60–120 are generally lower than the ones during hours 1–60; thus, the heating load is higher in the second period. The direct solar radiation hits the external window facade of rooms 1 and 2 from a west direction, the facade of room 4 from a south direction, the window facades of rooms 5 and 6 from an east direction and the north-oriented facade of room 3 is not hit by direct sunlight. During the occupancy periods, there is one person in rooms 3 and 5, two persons in rooms 1 and 6 and three persons in rooms 2 and 4.

In the first subplot of Fig. 7, the optimization trajectories for the CCA coupling variables in the form of the global control input $u_{\text{CCA,global}}$ and the local room copies $u_{\text{CCA,local},i}$ are presented. The ADMM applied to a non-convex problem performs well showing good convergence results. The trajectories of the global CCA control input and the local copies show a good agreement for almost the entire time horizon fulfilling the consensus constraint of one shared CCA control input. Some deviations can be found during hours 44, 50 and 100. The MAE between the local control input copies and the global CCA control input averaged over all subsystems is 0.001 and the RMSE is 0.001. The CCA is controlled with slow dynamics due to the high inertia and covers the heating base load which is generated by the slow disturbance quantity of the outdoor temperature. The first and fifth subplot show that the CCA supplies the highest mass flows before

the maximum heat demand at the time of the lowest outdoor temperatures; thus, the CCA is preheated to be able to cover the heating demand in a future period. By preheating the CCA, the time of energy supply and demand are decoupled. During the second warmer day, the CCA is hardly used and the convector nearly covers the entire heating load ("Heating power consumption" subplot).

As shown in the "Actuator mass flows" subplot, the convector is regulated in a more dynamic and responsive way and reacts to faster disturbances in the form of occupancy and solar radiation compensating for the heating peak loads. In contrast to the CCA, the maximum supply flows for the convector are provided at the time of the lowest outdoor temperatures. The maximum bounds for the mass flow to both CCA and convector (maximum mass flow of 0.1 kg/s) are met throughout the complete time horizon.

In the "Local temperatures" subplot it can be seen that thermal comfort can be ensured for almost the complete MPC horizon. Temperature bounds are exceeded during hours 24 and 120 leading to a total thermal discomfort of 3.03 Kh. The distributed MPC takes advantage of the comfort ranges during all periods and further cools down the rooms during the night set-back. During the period of high internal gains through occupancy and solar radiation (period of cooling load) the room temperatures are operated near the higher comfort bound and during the period of non-occupancy (period of heating load) the temperatures are kept very close to the lower comfort bound. In the power consumption subplots for the CCA, convector and artificial lighting the energy efficiency of the MPC approach is visible. During the periods of internal and solar gains, the heating power consumption is reduced to a low/ near-zero value. A widespread non-energy-efficient control phenomenon in buildings is simultaneous cooling and heating. The plots of the heating power consumption and Venetian blind control inputs ("Inclination angle" and "Shading position" subplot) reveal that cooling (here represented by the Venetian blinds to block solar heating energy from entering the room) and heating rarely occurs at the same time. Power is only consumed in periods where it is really needed. The total energy consumption of the distributed MPC approach is 683 668 kJ.

The Venetian blinds are controlled by regulating the vertical shading position and inclination angle to harvest a maximum of the cost-free solar heat gains and daylight ("Inclination angle" and "Shading position" subplot) and to predictively operate the room temperatures near the upper comfort bound. The missing illuminance to fulfill the illuminance set-points is provided by the artificial lighting ("Illumination power consumption" subplot).

In the "Inter-zone heat flows" subplot the impact of the door coupling compared to the wall coupling is depicted. The dimension of the heat flows induced by open door coupling is substantial compared to the wall-induced flows and generally higher (based on a door area of 1,9 m^2 and a wall area between the coupled rooms of 12 m^2). It confirms the thesis from Section 2 that open door coupling plays a major role in thermal coupling and should be taken into account.

In Fig. 8 a temperature plot for an exemplary local zone (here room 3, which is thermally coupled to three other rooms) is presented where both the optimized and simulated room temperature trajectories are plotted to validate the correct functionality of the MPC. The simulated and optimized trajectories match well which proves that the optimized trajectories calculated by the optimization solver show a good correlation with the ones obtained by applying the calculated control inputs to the coupled simulation model. It further implies that there are no essential unconsidered thermal heat flows induced by the neighbor rooms.

By applying the BLT decomposition scheme presented in Section 3, the number of algebraic variables, which form the largest fraction of the total variables, can be reduced significantly. For the example of the local optimization of room 1, the number of algebraic variables before the reduction is 480. By applying the decomposition scheme 434 algebraic variables can be eliminated resulting in 46 remaining algebraic variables which reduces the model size essentially. By using the BLT decomposition, the computation times can be reduced by up to 90 % compared to the original optimization problem with the full number of algebraic variables. The total number of variables for subproblem 1 is 95 including 33 inputs (4 control inputs, 1 slack variable, 24 disturbance variables and 4 communication variables of the distributed MPC), 3 time-varying parameters and 13 states. The computation time is 20 928 s and the computational time ratio is 0.048; accordingly, the distributed MPC approach is approximately 21 times faster than real-time.

In Fig. 9 the simulation results for the decentralized MPC variant are shown. The same BLT decomposition scheme as in the distributed MPC is applied. In the first subplot the simulated temperature trajectories are depicted. During most of the non-occupancy periods and at the beginning and end of the occupancy

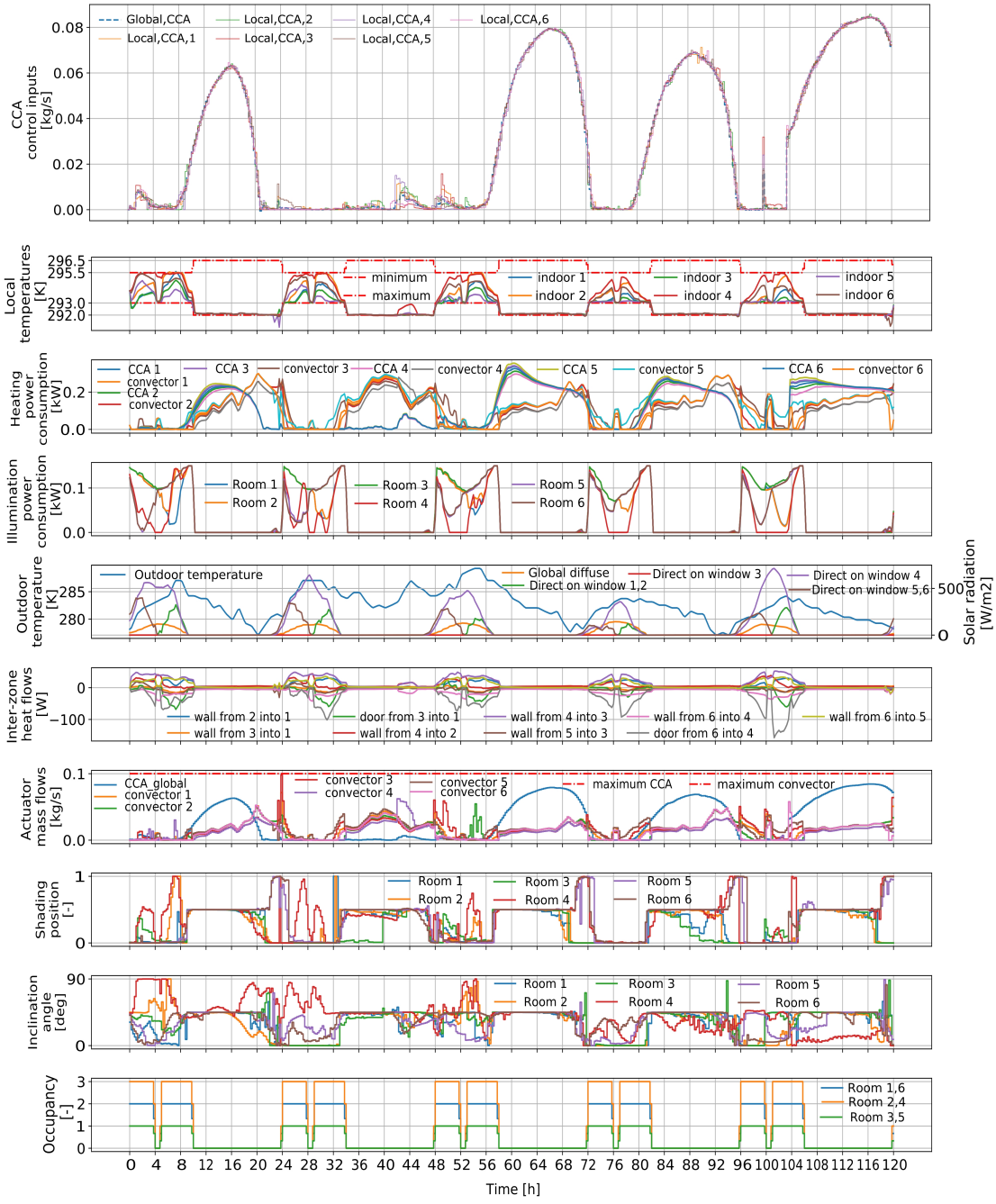

Figure 7: Simulation results of the distributed MPC

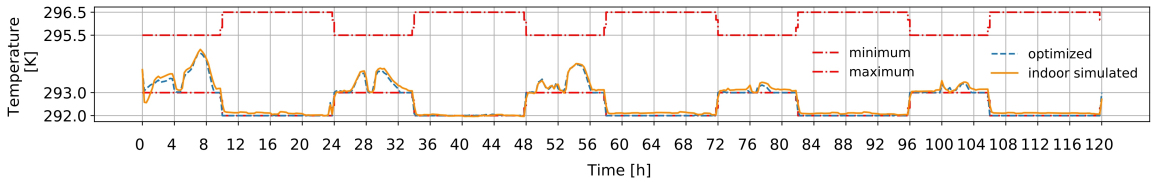

Figure 8: Optimized and simulated room temperature trajectories of room 3 for the distributed MPC

periods the lower comfort bounds of the rooms are violated. Neglecting thermal coupling and the inter-zone heat flows shown in the "Inter-zone heat flows" plot, heat flows leaving or entering the room towards other rooms are not taken into account which leads to constraint violations as the MPC tends to operate the temperatures near the bounds. The total thermal discomfort is 7.15 Kh. The convector is operated in a reactive and responsive way similar to the distributed MPC. However, the global CCA control input shows a less smooth control compared to the distributed approach displaying numerous sharp peaks which results in a control that is not appropriate for the inert CCA. The behavior is caused by the uncoordinated CCA control and averaging of all optimized CCA local control inputs before the simulation. Apart from this, the CCA trajectory hits the maximum bound during hours 60, 80–84 and 104–108. Neglecting any coupling in the disturbance quantities and cost function the decentralized MPC completely focuses on the minimization of local energy consumption resulting in an amount of 686 558 kJ, which is nevertheless slightly higher than for the distributed MPC due to the unconsidered inter-zone heat flows. Fig. 10 confirms the existence of high unconsidered inter-zone heat flows leading to a substantial mismatch between the optimized and simulated temperature trajectories for the exemplary room 3. The computation time of the decentralized MPC is 13 772 s with a computational time ratio of 0.032.

In Fig. 11 the simulation results for the centralized MPC variant are presented applying the same BLT decomposition as for the distributed and decentralized MPC. During the heating period, the room temperatures are operated more distant from the lower comfort bound compared to the distributed and decentralized approach leading to higher energy consumption of 818 130 kJ. Due to the high model complexity and number of optimization variables the optimization solver gets stuck in suboptimal local minima where the cost function result is significantly worse than for the distributed MPC. The local minima are further characterized by leaving the comfort bounds to a higher extent compared to the distributed MPC which results in a thermal discomfort amount of 6.18 Kh. In the "Heating power consumption" subplot it can be observed that, in contrast to the distributed and decentralized MPC, during the period of solar and internal gains there is still a high amount of consumed heating power. The mass flows supplied to the convector and CCA are rarely reduced to near zero and they are on a similar level near the middle of the control range for most of the prediction horizon. Additionally, the control of the central CCA mass flow contains some sharp peaks inducing an inapt CCA system control. The shading control shows a similar behavior compared to the CCA and convector mass flows and the control inputs are operated on a similar level in the midst of the control range for most of the time horizon. The computation time is 292 213 s with a computational time ratio of 0.676. Thus, the approach is not scalable and qualified for the real-time application of larger buildings.

The KPIs for all control concepts are summarized in Table 1. Compared to the decentralized variant, the energy consumption of the distributed variant is decreased by 0.4 % and the computation time is increased by 52.0 %. Thermal discomfort for the distributed MPC is significantly reduced by 57.6 % compared to the decentralized approach. Compared to the centralized optimization, the energy consumption for the distributed MPC is reduced by 16.4 % and discomfort is reduced by 51.0 %. The computation time is decreased substantially by 92.8 %.

To conclude, the application of the decentralized MPC results in an unacceptable amount of thermal discomfort and inappropriate CCA control whereas the centralized MPC leads to unacceptable high computation times, which renders the two variants as non-suitable approaches for a scalable, multi-zone building MPC. The proposed distributed MPC outperforms both approaches showing good convergence results for

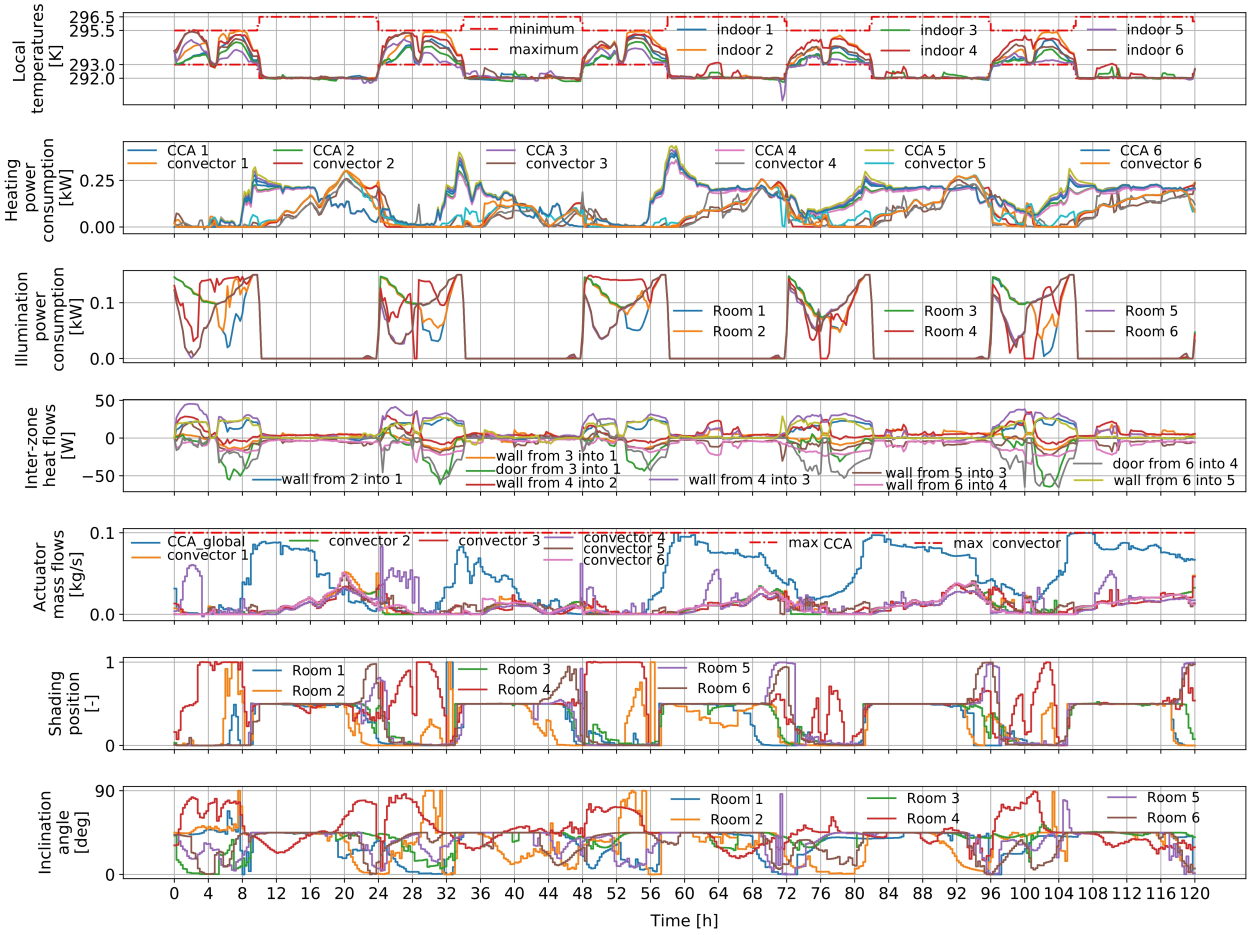

Figure 9: Simulation results of the decentralized MPC

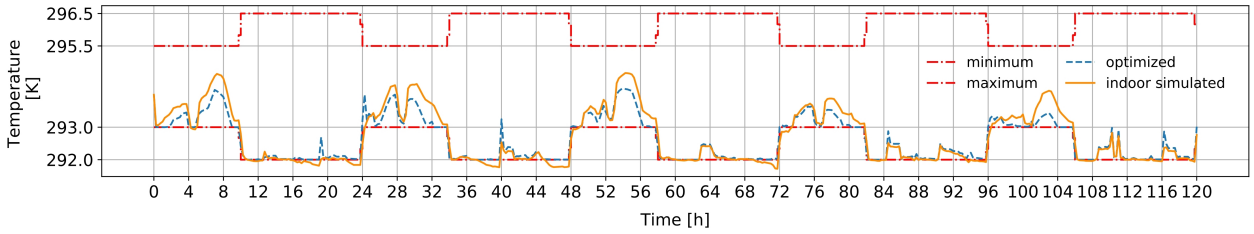

Figure 10: Optimized and simulated room temperature trajectories of room 3 for the decentralized MPC

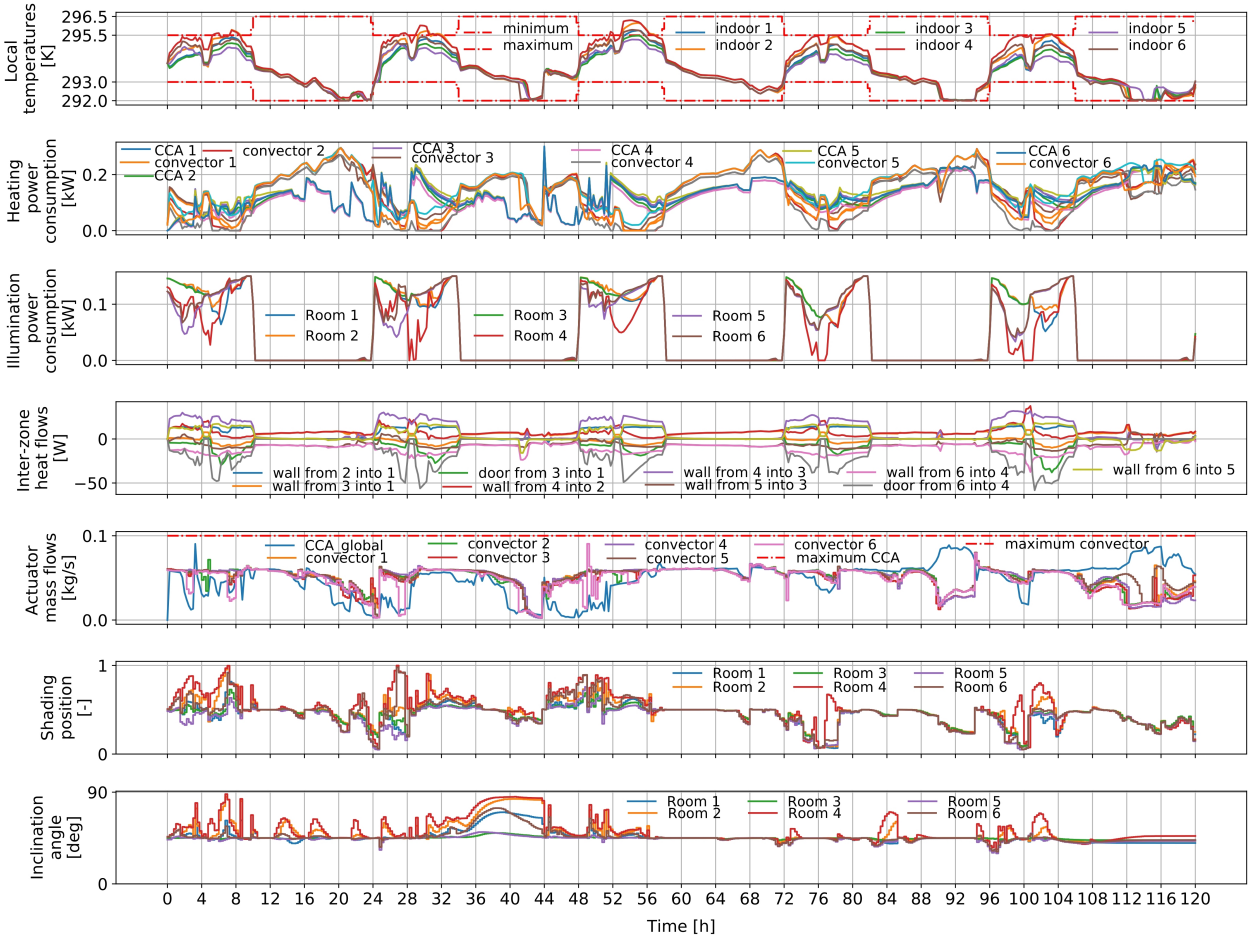

Figure 11: Simulation results of the centralized MPC

the ADMM and an adequate CCA control and is able to reduce thermal discomfort and computation time considerably while preserving high energy-efficiency. The case study has proven the potential as a suitable approach for the real-time MPC application for large-scale, multi-zone buildings.

	Energy consumption in kJ	Thermal discomfort in Kh	Computation time in s/ computational time ratio
Distributed approach	683 668	3.03	20 928/ 0.048
Decentralized approach	686 558	7.15	13 772/ 0.032
Centralized approach	818 130	6.18	292 213/ 0.676

Table 1: Comparison of KPIs for the different control approaches

5. Conclusion and outlook

In this paper, a distributed gradient-based MPC approach for large-scale, multi-zone building energy systems based on nonlinear Modelica controller models is presented. The proposed parallel and iterative approach addresses both thermal (thermal transfer between zones through walls and doors) and hydraulic coupling among different building zones (induced by a shared, central HVAC system). For considering thermal coupling, an uncooperative Nash optimization approach is chosen and for integrating hydraulic coupling, a cooperative approach based on a consensus ADMM is applied. Thermal coupling through doors is taken into account based on a data-driven, simulation-validated model, which calculates the air exchange between zones based on the room temperature difference. The local subsystem optimizations are coordinated and monitored by a central coordinator, which supports plug-n-play mechanisms based on the specified neighbor assignments.

In a simulative case study, the distributed MPC approach is applied to a nonlinear six-room-building Modelica model with detailed HVAC components, which accounts for both thermal and hydraulic TABS/ CCA coupling. The proposed control strategy is compared to centralized and decentralized MPC variants in terms of the KPIs energy consumption, thermal discomfort and computation time. The simulation results reveal that the distributed MPC approach outperforms both the centralized and decentralized variant reducing thermal discomfort by 57.6 % compared to the decentralized variant and reducing computation time by 92.8 % compared to the centralized variant. The consensus ADMM applied to the non-convex problem shows good convergence results yielding a low RMSE between the global CCA control input and the local room copies. The case study demonstrates the scalability and suitability of the distributed MPC approach for the control of large-scale buildings where the rooms are hydraulically coupled by TABS. It preserves a high energy efficiency and suits a real-time implementation being 21 times faster than real-time in the six-room use case. Applying a BLT decomposition method the number of algebraic variables of the subproblems can be reduced significantly leading to a substantial decrease in computation time.

Future planned extensions and improvements of the framework include an up-scaling to larger multi-zone buildings integrating further coupling constraints (e.g. maximum bounds for shared components), integration of the energy supply system, inclusion of integer decision variables, model calibration based on measurement data and the practical implementation of the approach.

Author contributions

Maximilian Mork: Conceptualization, Methodology, Software, Investigation, Writing - Original draft, Writing - Review & Editing, Visualization. André Xhonneux: Supervision, Writing - review & editing,

Project administration, Funding acquisition, Resources. Dirk Müller: Supervision, Writing - review & editing, Project administration, Funding acquisition, Resources.

Declaration of competing interest

The authors declare that they have no known competing financial interests or personal relationships that could have appeared to influence the work reported in this paper.

Acknowledgments

Funding: This work was supported by the BMWi (Federal Ministry for Economic Affairs and Energy), promotional reference 03EGB0010A.

References

[1] European Union, Directive (EU) 2018/844 of the European Parliament and of the Council of 30 May 2018 amending Directive 2010/31/EU on the energy performance of buildings and Directive 2012/27/EU on energy efficiency, Off. J. Eur. Union L 156 (2018) 75–91.
URL https://eur-lex.europa.eu/legal-content/EN/TXT/PDF/?uri=CELEX:32018L0844&from=EN

[2] European Commission, Commission Recommendation (EU) 2019/1019 of 7 June 2019 on building modernisation, Off. J. Eur. Union L165 (2019) 70–128.
URL https://eur-lex.europa.eu/legal-content/EN/TXT/PDF/?uri=CELEX:32019H1019&from=EN

[3] European Commission, The European green deal: communication from the commission to the European Parliament. the European Council, the Council, the European Economic and Social Committee and the Committee of the Regions (2019) 1–24.
URL https://eur-lex.europa.eu/legal-content/EN/TXT/?uri=CELEX:52019DC0640

[4] M. W. Ahmad, M. Mourshed, B. Yuce, Y. Rezgui, Computational intelligence techniques for HVAC systems: A review, Build. Simul. 9 (2016) 359–398. doi:10.1007/s12273-016-0285-4.

[5] International Energy Agency, Building Energy Performance Metrics- Supporting Energy Efficiency Progress in Major Economies (2015) 1–110.
URL http://www.buildingrating.org/sites/default/files/1448011796IEA_IPEEC_BEET4_Final_Report.pdf

[6] A. Afram, F. Janabi-Sharifi, Theory and applications of HVAC control systems - A review of model predictive control (MPC), Build. Environ. 72 (2014) 343–355. doi:10.1016/j.buildenv.2013.11.016.

[7] G. Serale, M. Fiorentini, A. Capozzoli, D. Bernardini, A. Bemporad, Model Predictive Control (MPC) for enhancing building and HVAC system energy efficiency: Problem formulation, applications and opportunities, Energies 11 (3, 631) (2018). doi:10.3390/en11030631.

[8] M. Killian, M. Kozek, Ten questions concerning model predictive control for energy efficient buildings, Build. Environ. 105 (2016) 403–412. doi:10.1016/j.buildenv.2016.05.034.

[9] M. Kavgic, T. Hilliard, L. Swan, Opportunities for implementation of MPC in commercial buildings, Energy Procedia 78 (2015) 2148–2153. doi:10.1016/j.egypro.2015.11.300.

[10] P. Höppe, Different aspects of assessing indoor and outdoor thermal comfort, Energy Build. 34 (6) (2002) 661–665. doi:10.1016/S0378-7788(02)00017-8.

[11] Y. Ma, A. Kelman, A. Daly, F. Borrelli, Predictive control for energy efficient buildings with thermal storage: Modeling, stimulation, and experiments, IEEE Control Syst. 32 (1) (2012) 44–64. doi:10.1109/MCS.2011.2172532.

[12] J. Cigler, D. Gyalistras, J. Siroky, V.-N. Tiet, L. Ferkl, Beyond Theory: the Challenge of Implementing Model Predictive Control in Buildings, in: 11th REHVA world Congr. 8th Int. Conf. Energy Effic. Smart Heal. Build., 2013, pp. 1008–1018.

[13] S. R. West, J. K. Ward, J. Wall, Trial results from a model predictive control and optimisation system for commercial building HVAC, Energy Build. 72 (2014) 271–279. doi:10.1016/j.enbuild.2013.12.037.

[14] S. C. Bengea, A. D. Kelman, F. Borrelli, R. Taylor, S. Narayanan, Implementation of model predictive control for an HVAC system in a mid-size commercial building, HVAC R Res. 20 (1) (2014) 121–135. doi:10.1080/10789669.2013.834781.

[15] R. De Coninck, L. Helsen, Practical implementation and evaluation of model predictive control for an office building in Brussels, Energy Build. 111 (2016) 290–298. doi:10.1016/j.enbuild.2015.11.014.

[16] D. Sturzenegger, D. Gyalistras, M. Morari, R. S. Smith, Model Predictive Climate Control of a Swiss Office Building: Implementation, Results, and Cost-Benefit Analysis, IEEE Trans. Control Syst. Technol. 24 (1) (2016) 1–12. doi:10.1109/TCST.2015.2415411.

[17] J. Drgoňa, L. Helsen, Different Problem Classes and Solution Techniques for Model Predictive Building Control, in: Proc. REHVA Annu. Meet. Conf. Low Carbon Technol. HVAC, Brussels, Belgium, 2018.

[18] R. P. Menon, F. Amblard, J. Page, Distributed Model Predictive Control for Demand Response on Thermal Devices in Building Blocks, in: Proc. 2019 IEEE PES Innov. Smart Grid Technol. Eur. ISGT-Europe, IEEE, 2019. doi:10.1109/ISGTEurope.2019.8905624.

[19] J. Drgoňa, J. Arroyo, I. Cupeiro Figueroa, D. Blum, K. Arendt, D. Kim, E. P. Ollé, J. Oravec, M. Wetter, D. L. Vrabie, L. Helsen, All you need to know about model predictive control for buildings, Annu. Rev. Control 50 (2020) 190–232. doi:10.1016/j.arcontrol.2020.09.001.

[20] S. Koehler, C. Danielson, F. Borrelli, A primal-dual active-set method for distributed model predictive control, Optim. Control Appl. Methods 38 (3) (2017) 399–419. doi:10.1002/oca.2262.

[21] P. D. Moroşan, R. Bourdais, D. Dumur, J. Buisson, A distributed MPC strategy based on Benders' decomposition applied to multi-source multi-zone temperature regulation, J. Process Control 21 (5) (2011) 729–737. doi:10.1016/j.jprocont.2010.12.002.

[22] S. Boyd, L. Xiao, A. Mutapcic, J. Mattingley, Notes on Decomposition Methods (2008).
URL https://see.stanford.edu/materials/lsocoee364b/08-decomposition_notes.pdf

[23] Y. Ma, G. Anderson, F. Borrelli, A distributed predictive control approach to building temperature regulation, in: Proc. 2011 Am. Control Conf., IEEE, San Francisco, CA, USA, 2011, pp. 2089–2094. doi:10.1109/acc.2011.5991549.

[24] Y. Long, S. Liu, L. Xie, K. H. Johansson, A scenario-based distributed stochastic MPC for building temperature regulation, in: 2014 IEEE Int. Conf. Autom. Sci. Eng., IEEE, New Taipei, Taiwan, 2014, pp. 1091–1096. doi:10.1109/CoASE.2014.6899461.

[25] R. Eini, S. Abdelwahed, Distributed Model Predictive Control based on Goal Coordination for Multi-zone Building Temperature Control, in: IEEE Green Technol. Conf., IEEE, Lafayette, LA, USA, 2019. doi:10.1109/GreenTech.2019.8767123.

[26] V. Putta, D. Kim, J. Cai, J. Hu, J. Braun, W. Lafayette, U. States, W. Lafayette, U. States, Distributed Model Predictive Control for Building HVAC systems : A Case Study., in: Int. High Perform. Build. Conf., 2014.
URL http://docs.lib.purdue.edu/ihpbc/150/

[27] H. F. Scherer, M. Pasamontes, J. L. Guzmán, J. D. Álvarez, E. Camponogara, J. E. Normey-Rico, Efficient building energy management using distributed model predictive control, J. Process Control 24 (6) (2014) 740–749. doi:10.1016/j.jprocont.2013.09.024.

[28] N. Radhakrishnan, Y. Su, R. Su, K. Poolla, Token based scheduling for energy management in building HVAC systems, Appl. Energy 173 (2016) 67–79. doi:10.1016/j.apenergy.2016.04.023.

[29] M. Baranski, J. Fütterer, D. Müller, Distributed exergy-based simulation-assisted control of HVAC supply chains, Energy Build. 175 (2018) 131–140. doi:10.1016/j.enbuild.2018.07.006.

[30] M. Baranski, L. Meyer, J. Fütterer, D. Müller, Comparative study of neighbor communication approaches for distributed model predictive control in building energy systems, Energy 182 (2019) 840–851. doi:10.1016/j.energy.2019.06.037.

[31] A. Kümpel, M. Baranski, D. Müller, Hierarchical multi-agent control of HVAC systems, in: ECOS 2019 - Proc. 32nd Int. Conf. Effic. Cost, Optim. Simul. Environ. Impact Energy Syst., Wroclaw, Poland, 2019, pp. 1305–1314.

[32] P. D. Moroşan, R. Bourdais, D. Dumur, J. Buisson, Distributed model predictive control for building temperature regulation, in: Proc. 2010 Am. Control Conf., IEEE, Baltimore, MD, USA, 2010, pp. 3174–3179. doi:10.1109/acc.2010.5530977.

[33] S. Roshany-Yamchi, K. Witheepanich, J. M. Escano, A. McGibney, S. Rea, Selective distributed model predictive control for comfort satisfaction in multi-zone buildings, in: 2017 21st Int. Conf. Syst. Theory, Control Comput., IEEE, Sinaia, Romania, 2017, pp. 648–653. doi:10.1109/ICSTCC.2017.8107109.

[34] X. Chen, Centralized and Distributed Identified Model Based Predictive Control for Museum Hermitage Amsterdam, 2019.
URL http://publications.pvandenhof.nl/MScThesis/XuChen_MSc_22-03-2019.pdf

[35] S. Boyd, N. Parikh, E. Chu, B. Peleato, J. Eckstein, Distributed optimization and statistical learning via the alternating direction method of multipliers, Found. Trends Mach. Learn. 3 (1) (2010) 1–122. doi:10.1561/2200000016.

[36] Q. Liu, X. Shen, Y. Gu, Linearized ADMM for Nonconvex Nonsmooth Optimization with Convergence Analysis, IEEE Access 7 (2019) 76131–76144. doi:10.1109/ACCESS.2019.2914461.

[37] Z. Xu, S. De, M. Figueiredo, C. Studer, T. Goldstein, An Empirical Study of ADMM for Nonconvex Problems (2016).
URL http://arxiv.org/abs/1612.03349

[38] T. Erseghe, Distributed optimal power flow using ADMM, IEEE Trans. Power Syst. 29 (5) (2014) 2370–2380. doi:10.1109/TPWRS.2014.2306495.

[39] A. Engelmann, Y. Jiang, T. Muhlpfordt, B. Houska, T. Faulwasser, Toward distributed OPF using ALADIN, IEEE Trans. Power Syst. 34 (1) (2019) 584–594. doi:10.1109/TPWRS.2018.2867682.

[40] B. Houska, Y. Jiang, Distributed Optimization and Control with ALADIN, in: Recent Adv. Model Predict. Control. Lect. Notes Control Inf. Sci., Vol. 485, Springer, Cham, 2021, pp. 135–163. doi:10.1007/978-3-030-63281-6_6.

[41] J. Cai, D. Kim, R. Jaramillo, J. E. Braun, J. Hu, A general multi-agent control approach for building energy system optimization, Energy Build. 127 (2016) 337–351. doi:10.1016/j.enbuild.2016.05.040.

[42] J. Cai, J. E. Braun, D. Kim, J. Hu, A multi-agent control based demand response strategy for multi-zone buildings, in: Proc. Am. Control Conf., IEEE, Boston, MA, USA, 2016, pp. 2365–2372. doi:10.1109/ACC.2016.7525271.

[43] X. Hou, Y. Xiao, J. Cai, J. Hu, J. E. Braun, Distributed model predictive control via Proximal Jacobian ADMM for building control applications, in: Proc. Am. Control Conf., IEEE, Seattle, WA, USA, 2017, pp. 37–43. doi:10.23919/ACC.2017.7962927.

[44] F. Lin, V. Adetola, Flexibility characterization of multi-zone buildings via distributed optimization, in: 2018 Annu. Am. Control Conf., IEEE, Milwaukee, WI, USA, 2018, pp. 5412–5417. doi:10.23919/ACC.2018.8431400.

[45] Y. Yang, G. Hu, C. J. Spanos, HVAC Energy Cost Optimization for a Multizone Building via a Decentralized Approach, IEEE Trans. Autom. Sci. Eng. 17 (4) (2020) 1950–1960. doi:10.1109/TASE.2020.2983486.

[46] W. Boydens, L. Helsen, B. W. Olesen, J. Laverge, Renewable and Storage-integrated Systems to Supply Comfort in

Buildings, A & S/books on Architecture and Arts, 2021. doi:10.5281/zenodo.5109932.
URL http://hdl.handle.net/1854/LU-8716306
[47] M. Killian, B. Mayer, M. Kozek, Cooperative fuzzy model predictive control for heating and cooling of buildings, Energy Build. 112 (2016) 130–140. doi:10.1016/j.enbuild.2015.12.017.
[48] S. E. Mattsson, H. Elmqvist, Modelica - An International Effort to Design the Next Generation Modeling Language, IFAC Proc. Vol. 30 (4) (1997) 151–155. doi:10.1016/s1474-6670(17)43628-7.
[49] G. Schweiger, R. Heimrath, B. Falay, K. O'Donovan, P. Nageler, R. Pertschy, G. Engel, W. Streicher, I. Leusbrock, District energy systems: Modelling paradigms and general-purpose tools, Energy 164 (2018) 1326–1340. doi:10.1016/j.energy.2018.08.193.
[50] M. Wetter, C. Van Treeck, New Generation Computational Tools for Building and Community Energy Systems Annex 60 Final Report, 2017.
URL http://www.iea-annex60.org/downloads/iea-ebc-annex60-final-report.pdf
[51] J. Åkesson, K. E. Årzén, M. Gäfvert, T. Bergdahl, H. Tummescheit, Modeling and optimization with Optimica and JModelica.org-Languages and tools for solving large-scale dynamic optimization problems, Comput. Chem. Eng. 34 (11) (2010) 1737–1749. doi:10.1016/j.compchemeng.2009.11.011.
[52] D. Müller, M. Lauster, A. Constantin, M. Fuchs, P. Remmen, Aixlib - an Open-Source Modelica Library Within the IEA-EBC Annex 60 Framework, in: Proc. CESBP Cent. Eur. Symp. Build. Phys. BauSIM 2016, Dresden, Germany, 2016, pp. 3–9.
[53] A. Wächter, L. T. Biegler, On the implementation of an interior-point filter line-search algorithm for large-scale nonlinear programming, Math. Program. 106 (1) (2006) 25–57. doi:10.1007/s10107-004-0559-y.
[54] M. Mork, A. Xhonneux, D. Müller, Hierarchical Model Predictive Control for complex building energy systems, Bauphysik 42 (6) (2020) 306–314. doi:10.1002/bapi.202000031.
[55] J. Drgoňa, D. Picard, L. Helsen, Cloud-based implementation of white-box model predictive control for a GEOTABS office building: A field test demonstration, J. Process Control 88 (2020) 63–77. doi:10.1016/j.jprocont.2020.02.007.
[56] F. Pedregosa, G. Varoquaux, A. Gramfort, V. Michel, B. Thirion, O. Grisel, M. Blondel, P. Prettenhofer, R. Weiss, V. Dubourg, J. Vanderplas, A. Passos, D. Cournapeau, M. Brucher, M. Perrot, E. Duchesnay, Scikit-learn: Machine Learning in Python, J. Mach. Learn. Res. 12 (2011) 2825–2830.
[57] F. Magnusson, J. Åkesson, Symbolic elimination in dynamic optimization based on block-triangular ordering, Optim. Methods Softw. 33 (1) (2018) 92–119. doi:10.1080/10556788.2016.1270944.
[58] HSL. A collection of Fortran codes for large scale scientific computation. (2013).
URL http://www.hsl.rl.ac.uk/